PROCEEDINGS OF SCIENCE

Measurements of ttbar+X using the ATLAS detector

Olga Bessidskaia Bylund*
Stockholm University
E-mail: olga.bylund@cern.ch
On behalf of the ATLAS Collaboration

The large integrated luminosity provided by the LHC enables the production of significant numbers of top quark pairs in association with additional jets or additional gauge bosons. The production of top quark pairs in association with W and Z bosons is presented. The measurement uses events with multiple leptons and in particular probes the coupling between the top quark and the Z boson. A significance of five standard deviations is found for the production of a top quark pair with a W boson. The cross section measurement of photons produced in association with top quark pairs is presented. The measurement uses a data driven technique to extract the signal from the background and achieves a significance of greater than 5 standard deviations. In addition, the production cross section of top quark pairs in association with jets is presented. This process allows better understanding of QCD effects and is an important background to many searches for physics beyond the Standard Model.

The European Physical Society Conference on High Energy Physics
22–29 July 2015
Vienna, Austria

*Speaker.

PoS(EPS-HEP2015)321

1. Introduction

In this communication, the recent measurements by the ATLAS collaboration [1] of the production of a top quark pair ($t\bar{t}$) in association with a Z boson, a W boson, a photon (γ) or with jets are presented. These processes are collectively referred to as $t\bar{t}+X$ in this text. The text starts by an introduction to the measurements of top quark pair production in association with a vector boson (Z, W, γ), proceeds to describe the measurements in Sec. 2 and 3 and introduces and describes the measurement of $t\bar{t}+$jets in Sec. 4.

The couplings of the top quark to Z bosons and photons govern the production of $t\bar{t}Z/\gamma^*$ and $t\bar{t}\gamma$. These processes have been largely unexplored due to their high production thresholds and measuring them to a high precision would test whether the processes are well described by the Standard Model or if physics beyond the Standard Model (BSM) is needed to describe the experimental results.

Studying the interactions of the most massive particles could teach us more about electroweak symmetry breaking. There are several BSM scenarios that can be tested by measuring the production of top quark pairs in association with a vector boson. Under the assumption of that BSM physics enters at a very high energy scale that prevents the production of new particles at the LHC, BSM physics could yet modify the interactions of the Standard Model particles. In the approach of Effective Field Theory [2], the interactions can be parametrized by a set of operators describing the additional interactions. The processes $t\bar{t}Z/\gamma^*$ and $t\bar{t}\gamma$ are sensitive to several such operators, as illustrated in Fig. 1 with the effect of new physics denoted by a blob. Some composite Higgs models predict heavy partners to the top quark of charge $+5/3e$ [3]. The presence of such particles would result in an enhancement of $t\bar{t}W$ production where this would be a stage in the decay chain $pp \to T^{5/3}\bar{t}$, $T^{5/3} \to tW^+$.

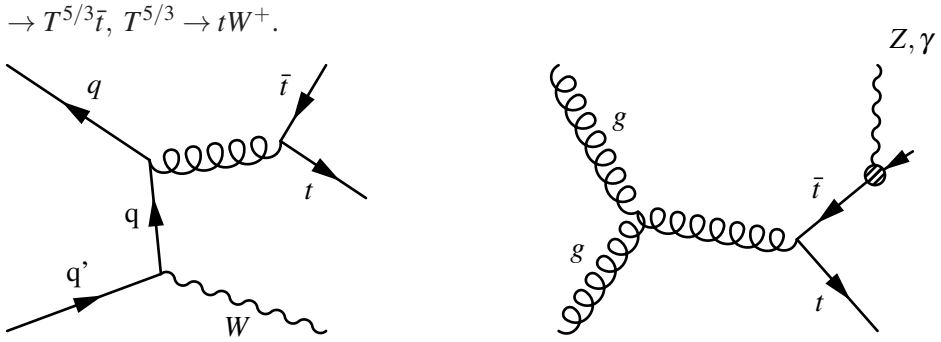

Figure 1: Example Feynman diagrams for the production of $t\bar{t}W$, $t\bar{t}Z$ and $t\bar{t}\gamma$. At leading order in the Standard Model, Z and γ bosons can be produced from the final state, while the W can not. The blob in the diagram to the right indicates the interaction vertex that could be modified by BSM physics.

2. Measuring $t\bar{t}Z/\gamma^*$ and $t\bar{t}W$

The $t\bar{t}Z/\gamma^*$ and $t\bar{t}W$ processes are measured in a simultaneous likelihood fit to ATLAS data collected at a centre of mass energy of $\sqrt{s} = 8\,\text{TeV}$, using the full 2012 dataset with an integrated luminosity of $\int L\,dt = 20.3\,\text{fb}^{-1}$ [4]. Four signal regions are defined for the analysis: opposite sign (OS) dilepton, same sign (SS) dilepton, trilepton and tetralepton. The SS dilepton region targets $t\bar{t}W$, the tetralepton region targets $t\bar{t}Z/\gamma^*$ while OS dilepton and trilepton target both processes.

The four signal regions are further split into many subregions, defined by cuts on missing transverse momentum $E_{\mathrm{T}}^{\mathrm{miss}}$, the invariant mass of lepton pairs m_{ll} and by the multiplicity of jets matched to b quarks (b-tagged jets). Each subregion is optimized individually to increase the sensitivity to the signal processes. Most subregions are optimized for either $t\bar{t}W$ or $t\bar{t}Z$, with the distinction created in general by either requiring or vetoing an opposite sign same flavour (OSSF) lepton pair with an invariant mass within 10 GeV of the mass of the Z boson.

The leptons that are targeted in the selection of the analysis are the ones originating from the vector bosons shown in Fig. 1 or from the W bosons produced in the decay of top quarks $t \to Wb$. Leptons originating from sources such as b-jets and photon conversions as well as other objects mistaken for leptons are referred to as fake leptons in this text. The charge of the selected leptons can also be misidentified (misID). Fake and charge misID leptons constitute the main background to the $t\bar{t}W$ search. The fake factor method and the matrix method are employed to estimate these backgrounds and cuts on tracks and impact parameters are applied to suppress their contribution.

For the subregions that target $t\bar{t}Z/\gamma^*$, the main background comes from diboson production, WZ or ZZ. The cross sections for these processes are determined in the likelihood fit, making use of dedicated control regions enriched in these processes. Figure 2 shows the different signal and control regions after the likelihood fit.

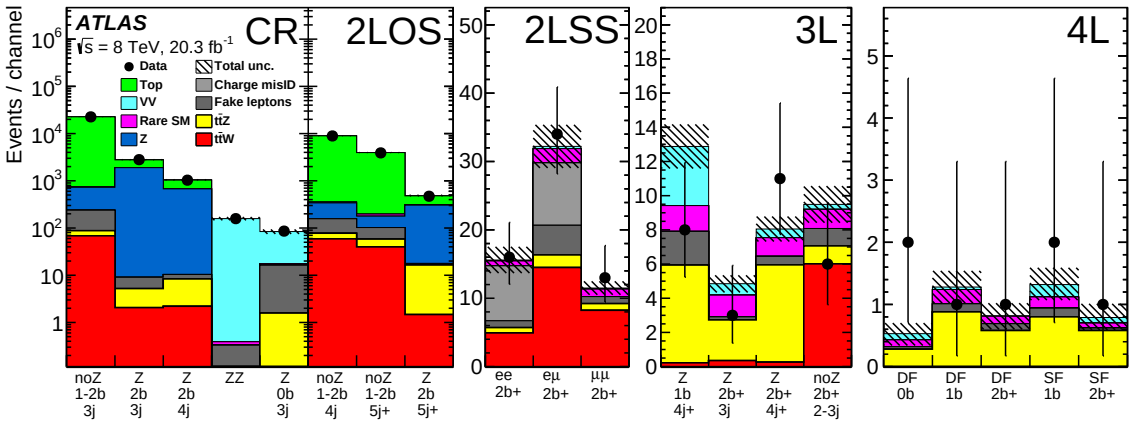

Figure 2: The yields after the likelihood fit in the four signal regions and the control regions (CR). The signal processes are shown in red for $t\bar{t}W$ and in yellow for $t\bar{t}Z/\gamma^*$ [4].

The measured cross sections are 369^{+86}_{-79}(stat.)$\pm$44(syst.)fb for $t\bar{t}W$ and 176^{+52}_{-48}(stat.)$\pm$24(syst.) fb for $t\bar{t}Z/\gamma^*$. The results are in agreement with the prediction of the Standard Model at next leading order (NLO) of $\sigma_{t\bar{t}W} = 232 \pm 32$ fb, $\sigma_{t\bar{t}Z/\gamma^*} = 215 \pm 30$ fb, obtained from MADGRAPH [5] interfaced with PYTHIA [6]. The statistical uncertainty is found to dominate the measurement. A profile likelihood tenchique is employed to evaluate the systematic uncertainties, which enter as nuisance parameters in the likelihood fit. The main systematic uncertainties originate from misidentified or charge misID leptons for the $t\bar{t}W$ cross section, and from background modeling for $t\bar{t}Z/\gamma^*$.

The significance of excluding the null hypothesis is shown in Table 1 region by region. The background only hypothesis is excluded by $5.0\,\sigma$ for $t\bar{t}W$ and by $4.2\,\sigma$ for $t\bar{t}Z/\gamma^*$. These numbers are derived from p-values for the simultaneous fit. The corresponding expected significance is

$3.2\,\sigma$ for $t\bar{t}W$ and $4.5\,\sigma$ for $t\bar{t}Z/\gamma^*$. The results show the first observation of $t\bar{t}W$ production and evidence by ATLAS of $t\bar{t}Z/\gamma^*$.

	$t\bar{t}W$ significance		$t\bar{t}Z$ significance	
Channel	Expected	Observed	Expected	Observed
2ℓOS	0.4	0.1	1.4	1.1
2ℓSS	2.8	5.0	-	-
3ℓ	1.4	1.0	3.7	3.3
4ℓ	-	-	2.0	2.4
Combined	3.2	5.0	4.5	4.2

Table 1: The significances, measured and expected, for the exclusion of the background only hypothesis decomposed into the different signal regions [4].

3. Measuring $t\bar{t}\gamma$

The $t\bar{t}\gamma$ analysis [7] presented here is performed using data collected by ATLAS at $\sqrt{s} = 7\,\text{TeV}$ and an integrated luminosity of $\int L\,dt = 4.59\,\text{fb}^{-1}$. The fiducial cross section, defined within the acceptance region of the detector and within the cuts used in the analysis, is measured using a template-based likelihood fit. The semileptonic decay mode of $t\bar{t}$ together with the production of an isolated photon, as illustrated in Fig. 3, is targeted. The signal events are simulated with MADGRAPH and WHIZARD [8] and interfaced with PYTHIA for the simulation of parton showering.

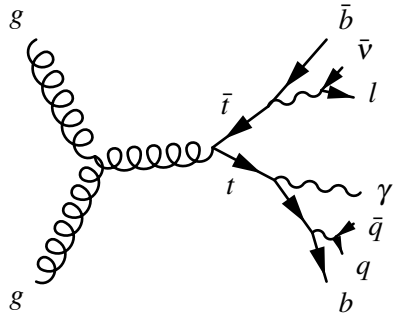

Figure 3: An example Feynman diagram illustrating the production of $t\bar{t}\gamma$, where $t\bar{t}$ decays to give exactly one lepton.

The selection requires at least one photon candidate with transverse energy $E_\text{T} > 20\,\text{GeV}$ together with at least four jets of which at least one is b-tagged. Additional cuts on e.g. isolation, E_T^miss and photon transverse momentum p_T are applied. To prevent the selection of events where electrons are misidentified as photons, a veto is applied against OSSF lepton pairs within 5 GeV of the mass of the Z boson.

The variable p_T^iso is the scalar sum of the p_T of the tracks in within a cone[1] around the photon candidate, and is a measure of its isolation. This variable is used to discriminate between prompt

[1]The size of this cone is $\Delta R = \sqrt{\Delta\phi^2 + \Delta\eta^2} = 0.2$, with ϕ being the azimuthal angle η the pseudorapidity.

photons and misidentified photons as well non-prompt photons originating from hadron decays. Templates for prompt and non-prompt or misidentified photons are derived from data. The distribution in $p_{\mathrm{T}}^{\mathrm{iso}}$ from the likelihood fit is shown in Fig. 4.

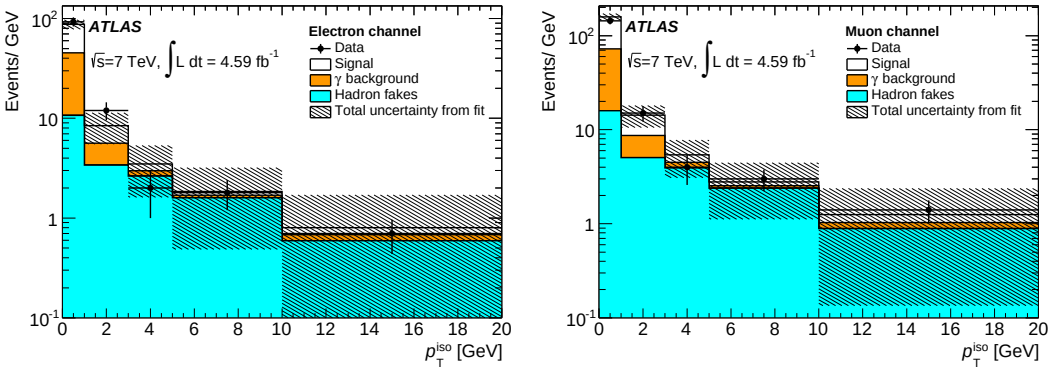

Figure 4: The distribution from the likelihood fit as a function of the discriminating variable p_{T}^{iso} for the electron channel (left) and the muon channel (right). The signal is shown in white. The main backgrounds are single photon production (orange) and fake leptons (blue) [7].

A profile likelihood fit is employed, with the systematic uncertainties entering as nuisance parameters. The main uncertainties relate to jet modeling, in particular to the jet energy scale, the photon modeling, the modeling of the signal and the *b*-tagging. The jet energy scale is determined by measuring the response of the detector to hadrons using testbeams and in-situ techniques [9]. For photon modeling, most of the uncertainty originates from photon identification [10]. The main systematic uncertainties are listed in Table 2.

Uncertainty source	Uncertainty [%]
Background template shapes	3.7
Signal template shapes	6.6
Signal modeling	8.4
Photon modeling	8.8
Lepton modeling	2.5
Jet modeling	16.6
b-tagging	8.2
$E_{\mathrm{T}}^{\mathrm{miss}}$ modeling	0.9
Luminosity	1.8
Background contributions	7.7

Table 2: The main systematic uncertainties for the $t\bar{t}\gamma$ measurement are presented here [7].

In total, 140 events with a single electron and 222 events with a single muon are selected. The number of signal $t\bar{t}\gamma$ events is determined with the likelihood fit to be 52 ± 14 in the electron channel and 100 ± 28 from the muon channel.

The null hypothesis is excluded by $5.3\,\sigma$. This is the first observation by ATLAS of the $t\bar{t}\gamma$ process. The fiducial cross section times the branching ratio is $\sigma_{t\bar{t}\gamma} \cdot BR = 63 \pm 8(\mathrm{stat})^{+17}_{-13}(\mathrm{syst}) \pm 1(\mathrm{lumi})$ fb for each lepton flavour, consistent with the Standard Model prediction of 48 ± 10 fb.

4. Measurements of $t\bar{t}+$jets

Through measurements of $t\bar{t}+$jets, higher order perturbative QCD effects can be studied and modeling uncertainties relating to $t\bar{t}$ radiation can be constrained. By understanding the behaviour at different jet multiplicities, the uncertainty on precision measurements of properties such as the top quark mass can be reduced. Additionally, $t\bar{t}+$jets production forms a background to many BSM searches.

The $t\bar{t}+$jets measurement is performed at $\sqrt{s} = 7\,\text{TeV}$, using the 2011 dataset with an integrated luminosity of $\int L\,dt = 4.6\,\text{fb}^{-1}$ [11]. The selection includes requirements on exactly one lepton (electron or muon) together with at least three jets, of which at least one is b-tagged. Various cuts on $E_{\text{T}}^{\text{miss}}$, $m_T(W)$ (the transverse mass of the charged lepton and $E_{\text{T}}^{\text{miss}}$) and jet p_{T} are applied. Fiducial differential cross sections as a function of jet p_{T} and jet multiplicity are measured. The strong coupling constant $\alpha_S(\mu_R)$ is varied to see which setting describes the data best.

Systematic uncertainties limit the precision, in particular background modeling at low jet multiplicities and the jet energy scale at high jet multiplicities. The main backgrounds are W+jets, single top and multijet. The normalisation of W+jets is extracted from data exploiting the charge asymmetry of leptons for this process. The single top background is determined from Monte Carlo simulations and the theoretical cross sections. The multijet background is assessed using the matrix method.

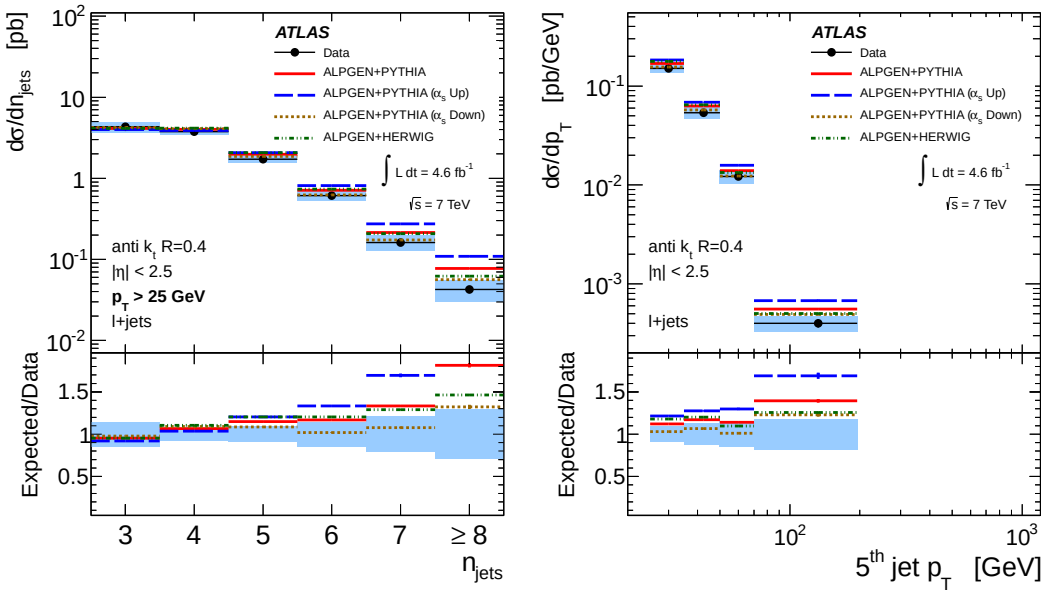

Figure 5: The jet multiplicity and the p_{T} of the first jet using ALPGEN+PYTHIA [11].

The strong coupling constant $\alpha_S(\mu_R)$ is varied by multiplying the renormalisation scale μ_R by a factor of 2 and a factor $1/2$ around the value $\mu_R = m_Z$, using ALPGEN [12] with PYTHIA. The results are shown in Fig. 5. Raising μ_R results in a lower α_S (denoted α_s Down) and lowering μ_R gives a higher α_S. In ALPGEN+PYTHIA, setting $\alpha_S(\mu_R = 2m_Z)$ is found to describe the data best.

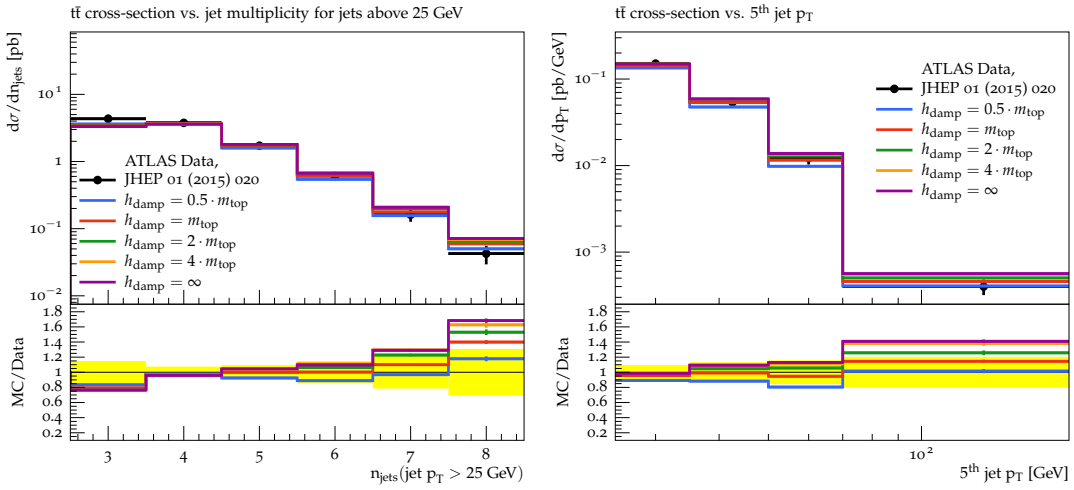

Figure 6: The resummation parameter h_{damp} in POWHEG is varied. The jet multiplicity is shown to the left and the p_{T} of the jet with the fifth highest p_{T} in an event is shown to the right [13].

In Monte Carlo simulations, jets are reconstructed either from partons introduced by the Matrix Element calculation of the process or from partons added to the event by the Sudakov parton showering procedures. Jets originating from the parton showering in general have a lower p_{T} that those originating from the Matrix Element calculation, as was observed in Ref. [11]. In the POWHEG generator [8], the resummation damping parameter h_{damp} that controls the matching can be used to tune the generated jet p_{T}. In this way, good agreement can be reached between data and simulation at high jet multiplicities when only at most one jet is simulated using the Matrix Element. The value of h_{damp} is varied in Ref. [13], generating $t\bar{t}$ at NLO using POWHEG and obtaining additional jets from the PYTHIA shower. Overall best agreement is found for $\mathrm{h_{damp}} = \mathrm{m_{top}}$, as seen in Fig. 6.

5. Conclusions

In conclusion, ATLAS has made the first observation of $t\bar{t}W$ at $\sqrt{s} = 8\,\mathrm{TeV}$ with the background only hypothesis excluded by $5.0\,\sigma$. The first observation by ATLAS of the $t\bar{t}\gamma$ process is performed at $\sqrt{s} = 7\,\mathrm{TeV}$, excluding the null hypothesis with $5.3\,\sigma$. Evidence of $t\bar{t}Z/\gamma^*$ production is found with the background excluded by $4.2\,\sigma$. The measured production cross sections for $t\bar{t}W$, $t\bar{t}Z/\gamma^*$ and $t\bar{t}\gamma$ are all found to be compatible with the Standard Model within estimated uncertainties. Moreover, studies are performed in $t\bar{t}+\mathrm{jets}$ production at $\sqrt{s} = 7\,\mathrm{TeV}$. It is found that the favoured value for $\alpha_S(\mu_R)$ corresponds to a value for the renormalization scale above the mass of the Z boson for the production of $t\bar{t}+\mathrm{jets}$. By using the resummation damping parameter h_{damp} in POWHEG and setting it to the mass of the top quark, one can describe the p_{T} of jets well while only simulating up to one jet by the computation of the Matrix Element. With these results in view, the ATLAS collaboration is looking forward to perform measurements at higher precision at $\sqrt{s} = 13\,\mathrm{TeV}$, testing the Standard Model and searching for signs of physics beyond the Standard Model.

References

[1] **ATLAS** Collaboration, "The ATLAS Experiment at the CERN Large Hadron Collider," *JINST* **3** (2008) S08003.

[2] A. Falkowski, "Effective field theory approach to LHC Higgs data," arXiv:1505.00046 [hep-ph].

[3] A. Azatov and J. Galloway, "Light Custodians and Higgs Physics in Composite Models," *Phys. Rev.* **D85** (2012) 055013, arXiv:1110.5646 [hep-ph].

[4] **ATLAS** Collaboration, "Measurement of the $t\bar{t}W$ and $t\bar{t}Z$ production cross sections in pp collisions at $\sqrt{s} = 8$ TeV with the ATLAS detector," arXiv:1509.05276 [hep-ex].

[5] J. Alwall, R. Frederix, S. Frixione, V. Hirschi, F. Maltoni, O. Mattelaer, H. S. Shao, T. Stelzer, P. Torrielli, and M. Zaro, "The automated computation of tree-level and next-to-leading order differential cross sections, and their matching to parton shower simulations," *JHEP* **07** (2014) 079, arXiv:1405.0301 [hep-ph].

[6] T. Sjostrand, S. Mrenna, and P. Z. Skands, "PYTHIA 6.4 Physics and Manual," *JHEP* **05** (2006) 026, arXiv:hep-ph/0603175 [hep-ph].

[7] **ATLAS** Collaboration, "Observation of top-quark pair production in association with a photon and measurement of the $t\bar{t}\gamma$ production cross section in pp collisions at $\sqrt{s} = 7$ TeV using the ATLAS detector," *Phys. Rev.* **D91** no.~7, (2015) 072007, arXiv:1502.00586 [hep-ex].

[8] W. Kilian, "WHIZARD manual," whizard.hepforge.org/manual.pdf.

[9] **ATLAS** Collaboration, "Jet energy measurement and its systematic uncertainty in proton-proton collisions at $\sqrt{s} = 7$ TeV with the ATLAS detector," *Eur. Phys. J.* **C75** (2015) 17, arXiv:1406.0076 [hep-ex].

[10] **ATLAS** Collaboration, "Measurements of the photon identification efficiency with the ATLAS detector using 4.9 fb^{-1} of pp collision data collected in 2011," Tech. Rep. ATLAS-CONF-2012-123, CERN, Geneva, Aug, 2012. cds.cern.ch/record/1473426.

[11] **ATLAS** Collaboration, "Measurement of the $t\bar{t}$ production cross-section as a function of jet multiplicity and jet transverse momentum in 7 TeV proton-proton collisions with the ATLAS detector," *JHEP* **01** (2015) 020, arXiv:1407.0891 [hep-ex].

[12] M. L. Mangano, M. Moretti, F. Piccinini, R. Pittau, and A. D. Polosa, "ALPGEN, a generator for hard multiparton processes in hadronic collisions," *JHEP* **07** (2003) 001, arXiv:hep-ph/0206293 [hep-ph].

[13] **ATLAS** Collaboration, "Comparison of Monte Carlo generator predictions from Powheg and Sherpa to ATLAS measurements of top pair production at 7 TeV," Tech. Rep. ATL-PHYS-PUB-2015-011, CERN, Geneva, May, 2015. cds.cern.ch/record/2020602.